JTE HCMUTE
ISSN: 2615-9740

JOURNAL OF TECHNICAL EDUCATION SCIENCE
Ho Chi Minh City University of Technology and Education
Website: https://jte.edu.vn
Email: jte@hcmute.edu.vn

Enhanced Teleoperation and Visual-Force Feedback with Obstacle Avoidance for a Car-like Mobile Robot based on WAN Network Architecture

Duc Thien Tran*, Hoang Quan Vo, Trung Kien Nguyen, Thanh Nha Nguyen
Ho Chi Minh City University of Technology and Education, Vietnam

*Corresponding author. *Email*: *thientd@hcmute.edu.vn*

ARTICLE INFO

Received: 22/05/2024
Revised: 20/07/2024
Accepted: 23/07/2024
Published: 28/02/2025

KEYWORDS

Car-like mobile robot;
Wide Area Network (WAN);
Teleoperation control;
Message Queuing Telemetry Transport (MQTT);
Obstacle avoidance.

ABSTRACT

This paper presents an enhanced teleoperation system and visual-force feedback with obstacle avoidance for a Car-like mobile robot. The proposed system includes a local station, a remote station, and a communication channel. The local station allows the operator to give acceleration, orientation, and driving mode commands. It generates the haptic effect of the obstacles in the remote station for the operator due to the visual-force feedback. The remote station is a Car-like mobile robot executing control commands from the local station and providing feedback on the working status of the robot. Moreover, the robot has the ability of obstacle avoidance through the Potential Field (PF) algorithm with input signals being the distance from the robot to obstacles and a virtual repulsive force that influences both the steering angle of the robot and the haptic steering wheel system. The communication channel will connect the local station and the remote station wirelessly based on Wide Area Network (WAN) architecture with the Message Queuing Telemetry Transport (MQTT) to resolve complex problems such as control distance, latency, etc. Several case studies are used to evaluate the efficacy of providing the operator with haptic and visual feedback at any control distance.

Doi: https://doi.org/10.54644/jte.2025.1601

1. Introduction

The advancement of technology is leading to an increased utilization of mobile robots in various fields and tasks, replacing human involvement. Two common control methods that many researchers focus on are autonomous navigation [1] and teleoperation control [2], each having its advantages and disadvantages. The Society of Automotive Engineers (SAE) defines five levels of autonomy for Car-like mobile robots. Achieving complete human intervention-free operation, known as level five (fully autonomous), comes with high computational costs. Fully autonomous systems [3] require sophisticated algorithms for precise control, and dealing with dynamic environments makes them less reliable without human intervention. For tasks requiring high precision, like search and rescue [4] operations or in agriculture [5] with constantly changing conditions, fully autonomous navigation faces significant challenges. As a result, recent developments focus on and continuously improve remote control systems for mobile robots.

Remote control systems for mobile robots allow humans to perceive the environment surrounding the robot from a distance and provide control commands. The main advantage of this system is enhanced work efficiency, which leverages human intelligence and experience while ensuring the absence of the controller in the working environment of the robot. However, the system is limited by communication accuracy, which depends on the control distance and system latency [6]. Additionally, human perception limitations regarding the working environment of the robot pose challenges in control. An Internet-based control system was employed for a wireless mobile robot, utilizing the Common Object Request Broker Architecture (CORBA) communication framework for remote control [7]. However, the system lacked a control chamber, hindering operators from gathering environmental data crucial for decision-making. Another mobile robot was operated via Radio Frequency (RF) waves, with interaction facilitated through a control interface [8]. But the operators encountered challenges due to the sole reliance on a button-

based interface without peripheral devices or sensory feedback. A Car-like mobile robot incorporated force feedback via tactile sensors and employed the Zigbee protocol for remote control [9]. This configuration enabled the driver of haptic feedback to avoid collisions. Nevertheless, these projects still faced with limitations such as restricted control range, limited visibility of the environment, and the absence of safety features for operators. From the limitations of the previous studies came the motivation for this paper to propose a combined approach to optimize the operation of mobile robots.

Based on the above analysis, this paper proposes a remote control system for car-like mobile robots over the WAN. The proposed system is designed with a local station and a remote station which is a car-like mobile robot. The high-level communication protocol MQTT is used for communication between the two entities on a cloud computing platform, 4 Generation (4G) Long Term Evolution (LTE), and Wireless Fidelity (Wifi). This allows the control range to be extended to the global level as long as the system is connected to the Internet. A force feedback steering wheel, a visual feedback user interface, and an obstacle avoidance feature based on the PF algorithm are also developed to enhance the controllability of the driver. Finally, experiments were conducted to evaluate the responsiveness of the system and the effectiveness of the method in terms of user controllability.

The remainder of this paper is structured as follows: section 2 provides an overview of the system, including four parts: local station, remote station, communication channel, and visual-force feedback. Section 3, the main part of this document, discusses the communication protocol between the local and remote stations. In Section 4, detailed explanations of the control methods at the local and remote stations are provided. Experimental cases of the remote control system are presented in Section 5. Section 6 provides the conclusion of this paper.

2. System description

The proposed system consists of two main components: the remote station and the local station. Both of them connect through a communication channel built as a WAN [10]. MQTT protocol is used to transfer data between the local station and the remote station [11]. The relationship between these two entities is illustrated in Figure 1.

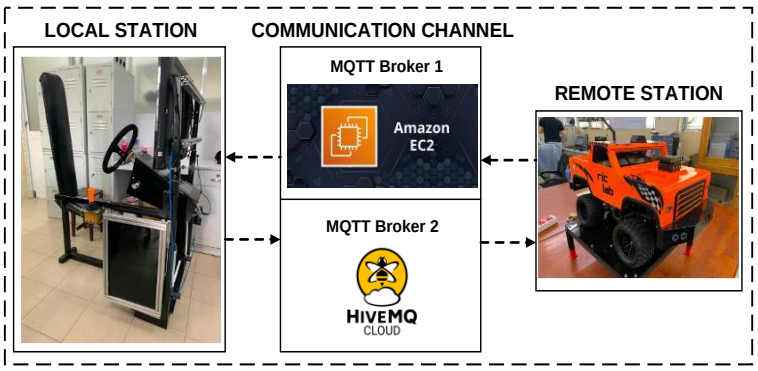

Figure 1. *Overview of the teleoperation car system*

2.1. Local station

The local station as depicted in Figure 2 is a stationary system designed for a user to control a mobile robot at the remote station through mechanisms similar to a car, including a human, haptic steering system, pedal sensor, mode stick, Graphic User Interface (GUI), and Electronic Control Units (ECU). The human gives the commands control to the ECU through the actuators. The ECU has two ESP32 modules: Master and Slave module. The Master module receives the commands control, and then encodes this commands into a message packet, and sends it to Broker 1. Besides that, the Master module is also involved in controlling the force feedback motor on the steering wheel thanks to the PF algorithm. The Slave module is used to receive feedback signals from the distance sensors of the remote station through Broker 1 and send them to the Master module for collision warning force feedback purposes. Additionally, a GUI display real-time images and sensor data of the robot from a remotely working environment for operators. The proposed system operates as a closed-loop system with the feedback signal from the camera module and distance sensors.

JTE
HCMUTE
ISSN: 2615-9740

JOURNAL OF TECHNICAL EDUCATION SCIENCE
Ho Chi Minh City University of Technology and Education
Website: https://jte.edu.vn
Email: jte@hcmute.edu.vn

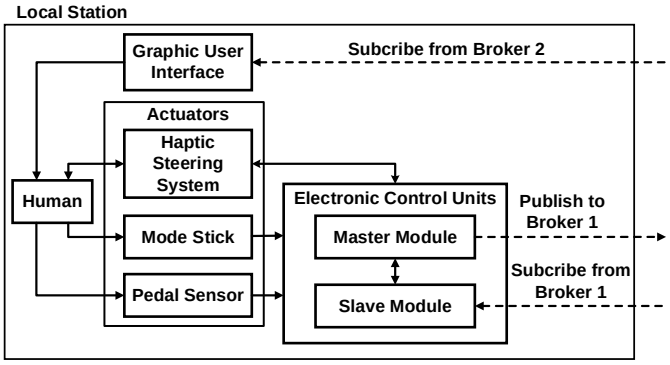

Figure 2. *Local station architecture*

2.2. Remote station

The remote station is a Car-like mobile robot remotely controlled from a specific distance. Consider a model similar to a car, as shown in Figure 3, with four wheels divided into two parts. The first part consists of two rear wheels fixed in parallel to the body of the vehicle. The remaining part includes two front steering wheels also parallel to each other. It can turn left or right at an angle but cannot immediately move sideways. Therefore, it is known as a non-holonomic system.

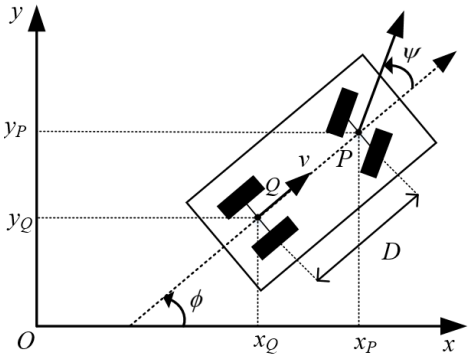

Figure 3. *The Car-like mobile robot kinematic model*

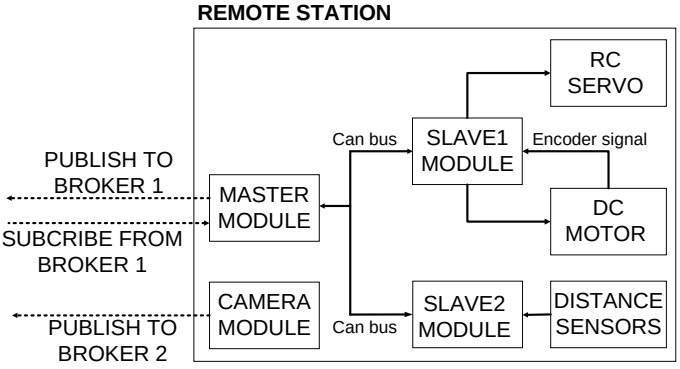

Figure 4. *Remote station architecture*

In this study, the detailed structure of the Car-like mobile robot is presented in Figure 4. This system included modules: Master, Slave1, Slave2, Camera, RC servo, DC motor, and distance sensors. Firstly, the Master module receives and decodes message packets from the local station through Broker1. After that, the Master module sends control signals to the Slave1 module for controlling the steering angle by RC servo and car speed by DC motor. Simultaneously, the Slave1 module reads the encoder signal of the DC motor to regulate the DC motor speed by the Proportional Integral Derivative (PID) controller. Lastly, the Slave2 module reads and then sends distance sensor data to the Master module. Both of the slave modules communicate with the Master module through a local network system called the Control Area Network (CAN) to ensure stability.

2.3. Communication channel

The global internet network serves as the wireless data transmission environment between the control station and the mobile robot based on the Transmission Control Protocol/Internet Protocol (TCP/IP) platform. The system is structured like a WAN, where the control station is Local Area Network (LAN) 1, and the mobile robot is LAN 2. Due to the mobility nature, a wireless cellular network is employed on the mobile robot, while a wireless wifi network is used at the control station. However, to ensure stability, optimization, and data security of the transmission, a high-level communication protocol MQTT is integrated.

2.4. Visual-force feedback

Image data feedback from the surrounding environment of the robot in a remote setting is collected through a built-in camera within the Car-like mobile robot. Subsequently, the data is processed, compressed, and transmitted to the control station. The received image data is then encoded, and the frame size is adjusted to match the user interface for visual feedback purposes. Information regarding obstacles is also gathered and displayed on the user interface as in Figure 5.

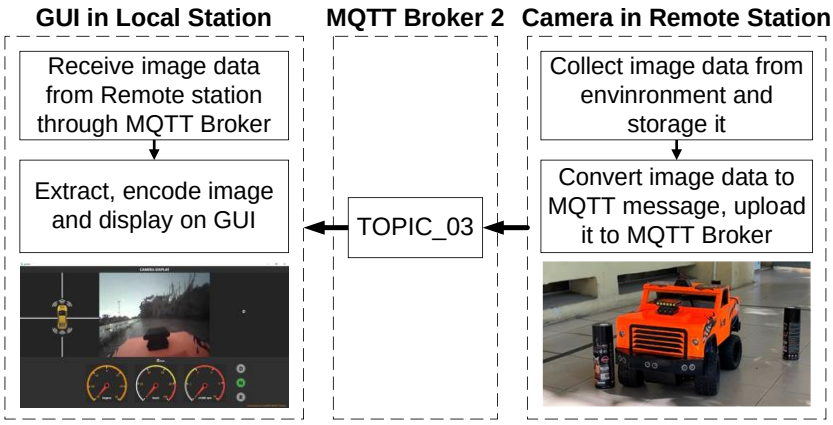

Figure 5. *Visual feedback on GUI in the local station*

The force feedback data is calculated based on distance data obtained in the working environment of the robot through ultrasonic sensors. Using the PF algorithm, the force coefficient is encoded into the feedback packet sent to the local station after the computation. Depending on the received force coefficient value, the force feedback on the steering wheel system will generate a haptic effect to alert the operator about obstacles ahead of the robot.

3. MQTT protocol

The MQTT protocol is designed to operate on unreliable and low-bandwidth networks, allowing IoT devices to send and receive messages with low latency, minimal resource consumption, and long distances between devices. As a high-level communication protocol, MQTT requires devices exchanging data to establish a proper sequence to ensure both data security and transmission speed.

In the proposed system, two intermediary MQTT broker servers have been established for the dual purposes of transmitting and receiving images and controlling commands, as well as receiving feedback information. These brokers are created by using the services of two different cloud computing providers: Amazon Web Services (AWS) for image data and HiveMQ for control and feedback data, aiming to optimize service costs.

3.1. MQTT protocol for transmitting controlling commands and receiving feedback data

HiveMQ broker is used for transmitting control commands and receiving feedback data. Establishing a two-way packet exchange between the control station and the mobile robot is necessary for both systems to participate in the MQTT protocol. The local station plays the role of client 1, remote station is client 2. They are both set up into two topics as subscriber and publisher as in Figure 6.

JTE HCMUTE
ISSN: 2615-9740
JOURNAL OF TECHNICAL EDUCATION SCIENCE
Ho Chi Minh City University of Technology and Education
Website: https://jte.edu.vn
Email: jte@hcmute.edu.vn

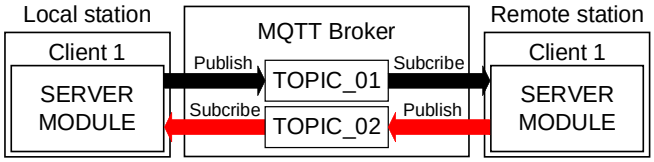

Figure 6. *MQTT Broker in HiveMQ Cloud*

3.2. MQTT protocol for visual feedback

To obtain live image data from the operating environment of the robot, the ESP32 Cam module was employed. This module is connected to the internet via a 4G cellular network, compressing the data and sending it to the MQTT broker. AWS cloud computing service is utilized for fast and accurate transmission of large-sized image data. The remote station plays the role of client 1 and publishes data to topic 1 of the MQTT broker. The GUI at the local station plays the role of client 2, subscribes to topic 1, and receives feedback data.

4. Control method

4.1. Local station

The flowchart presents the local station principle as in Figure 7.

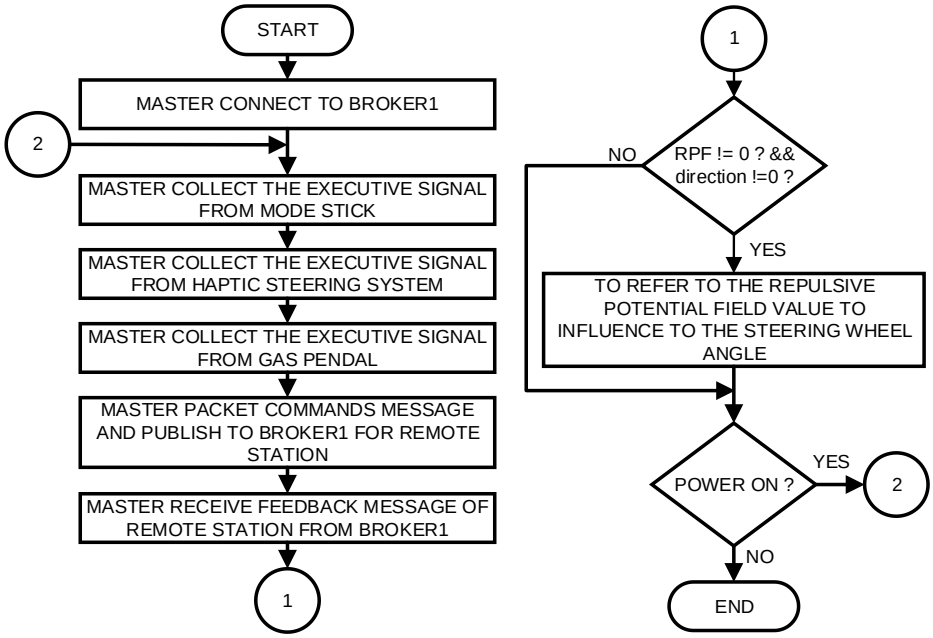

Figure 7. *The flowchart of the local station*

At the local station, a linear PID controller, represented by the formula (1), is employed to control the regeneration of the steering force and provide straight-line feedback to the steering wheel through two Direct Current (DC) motors.

$$u_1(t) = K_{p_1} e_1(t) + K_{i_1} \int_0^t e_1(\tau) d\tau + K_{d_1} \frac{d}{dt} e_1(t) \quad (1)$$

Where e_1 is the tracking error of the system (degree), K_{p_1} is the proportional gain, K_{i_1} is the internal gain, K_{d_1} is the derivative gain, and t is the sampling time for the system(s).

The tracking error of the system is defined as:

$$e_1 = q_d - q \quad (2)$$

With q_d representing the set value at 0 corresponding to the straight-ahead position, and q being the current steering wheel angle constrained.

At the moment of an imminent collision, the obstacle avoidance algorithm intervenes immediately. Subsequently, environmental data from the robot is transmitted back to the cockpit, and the force feedback algorithm is applied to the steering system based on the potential field repulsive force using the formula (3).

$$\Delta u = \begin{cases} K.U_{rep}(q), U_{rep}(q) > 0 \\ 0, U_{rep}(q) \le 0 \end{cases} \quad (3)$$

Where Δu represents the steering resistance of the steering system, K is the steering damping coefficient of the steering system, $U_{rep}(q)$ is the potential field repulsive force value of the robot system. If the potential field repulsive force value is larger, the steering system becomes heavier, hindering control. This also serves as a necessary warning to help the operator become aware of the impending collision with an obstacle.

4.2. Remote station

The remote station principle is presented in Figure 8.

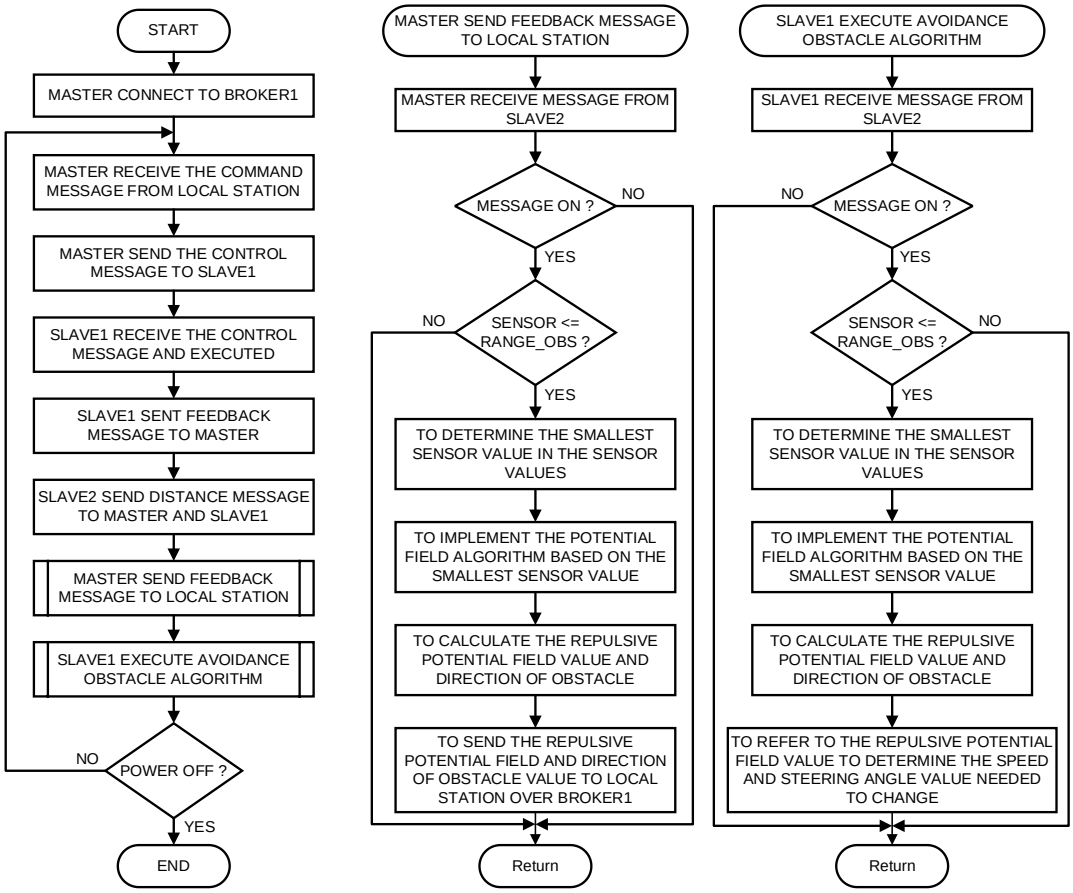

Figure 8. *The flowchart of the remote station*

Besides, the remote station operates through a CAN network system with 3 nodes as shown in the diagram. A PI controller is employed to control the speed of the DC encoder motor, as described in equation (4).

$$u_2(t) = K_{p_2} e_2(t) + k_{i_2} \int_0^t e_2(\tau) d\tau \quad (4)$$

Where e_2 is the tracking error of the system (RPM), K_{p_2} is the proportional gain, K_{i_2} is the internal gain.

The PF algorithm [12] is employed for the automated obstacle avoidance steering of the vehicle. When an obstacle enters the danger zone with a velocity greater than the dangerous velocity threshold, as defined by (5), the robot system at the remote station will enter an automatic obstacle avoidance state. After the obstacle avoidance process is complete, control authority is returned to the driver.

$$\begin{cases} D(q)_{\min} \le d_{threshold} \\ v \ge v_{threshold} \end{cases} \tag{5}$$

Where $D(q)_{\min}$ represents the distance from the robot to the nearest obstacle (cm). $d_{threshold}$ is the critical distance at which a collision might occur (cm). v is the current motor speed of the robot (rpm), and $v_{threshold}$ is the motor speed at which a collision might occur. The obstacle avoidance feature is based on the APF algorithm formula (6).

$$U_{rep}(q) = \begin{cases} \frac{1}{2}\xi\left(\frac{1}{D(q)} - \frac{1}{Q^*}\right)^2 & ,D(q) \le Q^* \\ 0 & ,D(q) > Q^* \end{cases} \tag{6}$$

Where $U_{rep}(q)$ is the repulsive field acting on the robot system at a distance q, ξ is the repulsion coefficient, $D(q)$ is the minimum distance from the robot system to the obstacle, and Q^* is the threshold distance of influence.

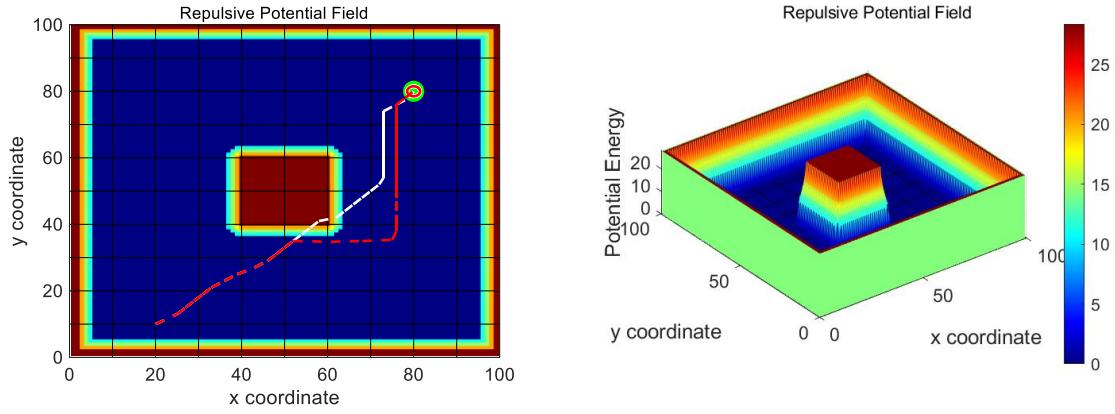

a) ***b)***

Figure 9. a) *The effectiveness of Repulsive PF on MATLAB; b) The level of Repulsive PF on MATLAB*

The results obtained after applying the obstacle avoidance algorithm include the repulsive force from the obstacle to the robot. This force affects the steering angle of the vehicle, with a larger repulsive force leading to a greater steering angle. Additionally, when there is a force from the potential field, the parameters of the Proportional Integral (PI) speed controller for the DC motor are adjusted to bring the vehicle speed to a suitable level for obstacle avoidance. The obstacle avoidance algorithm is simulated and fine-tuned using MATLAB software, resulting in values for the potential field force and the obstacle avoidance outcome as shown in Figure 9. When the potential field force is applied, the robot follows the path indicated by the red line, deviating from the collision with the obstacle on the motion path represented by the white line.

When operating in a real environment, to stabilize the ultrasonic sensor readings, the obtained values undergo noise filtering using a low-pass filter through a formula (7). The distance values to obstacles from the sensor after low-pass filtering are the input parameters for the obstacle avoidance feature using the PF algorithm.

JTE HCMUTE
ISSN: 2615-9740
JOURNAL OF TECHNICAL EDUCATION SCIENCE
Ho Chi Minh City University of Technology and Education
Website: https://jte.edu.vn
Email: jte@hcmute.edu.vn

$$u_{out}(t) = u_{in}(t) - \omega_0 \frac{du_{out}}{dt} \quad (7)$$

Where $u_{out}(t)$ is the signal from the sensor after the low-pass filter (cm), $u_{in}(t)$ is the signal from the sensor input to the low-pass filter (cm), ω_0 is the cutoff frequency of the low-pass filter, t is the current time, $\frac{du_{out}}{dt}$ is the signal from the sensor after the low-pass filter at the previous time t.

5. Test and results

5.1. Experiment to show the responsiveness of the system

An experiment was conducted to evaluate the responsiveness of the system. In this experiment, the driver turns the steering wheel to one side until it reaches the maximum limit and then back to the maximum of the opposite side. As soon as the driver releases the steering wheel slightly, the PID controller returns it to the center position. The responsiveness of the steering wheel is shown in Figure 10. The PID controller parameters are: q being the current steering wheel angle constrained within the range of [-540; 540], corresponding to steering the wheel 1.5 turns each way. The proportional gain is K_{p_1} = 0.75, the integral gain is K_{i_1} = 0.003, the derivative gain is K_{d_1} = 0.25, and the sampling time for the system is t = 0.01.

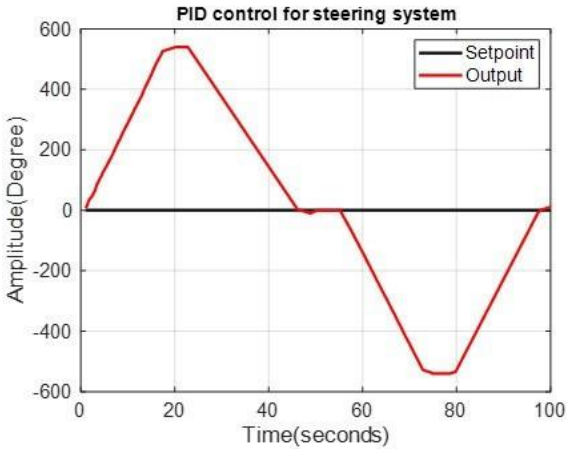

Figure 10. *PID control for steering system*

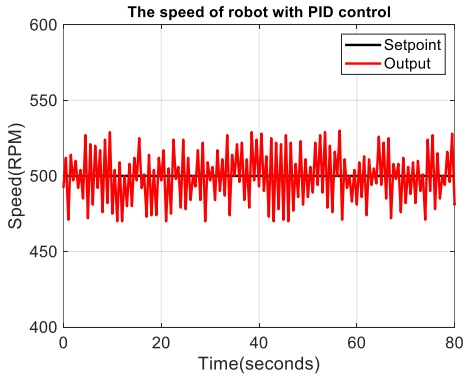

Figure 11. *The speed of robot with PI controller*

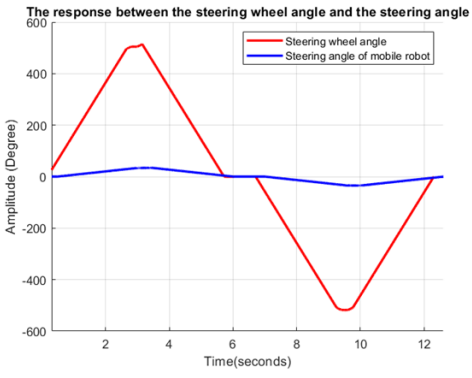

Figure 12. *The response between the steering wheel angle and the steering angle*

Following the steering wheel evaluation, the driver connected the control station directly to the mobile robot. They then performed steering maneuvers with various turning angles, observing the responsiveness of the robot. Simultaneously, the driver pressed the accelerator pedal to assess the influence of the PI controller on the behavior of the DC motor Figure 11. The PI controller parameter

has K_{p_2} =0.065 and K_{i_2} =0.16. Chart Figure 12 illustrates the responsiveness of the steering wheel rotation angle and the steering angle of the mobile robot. Based on this, the delay time of the teleoperation system is estimated to be between 0.1 and 0.3 seconds during the experiment process. However, it should be noted that the delay factor is contingent upon the Internet connection.

Through testing, the responsiveness of the system has been demonstrated. The steering mechanism with the PID controller provides power assistance for the driver. The responsiveness between the steering wheel angle and the steering angle on the robot is proven. The applied PI controller helps the motor speed closely track the set speed, reducing overshoot and improving stability.

5.2. Experiment to show the effectiveness of the system force feedback feature.

To demonstrate the enhanced features of the remote control system for the Car-like mobile robot, incorporating visual feedback and haptic feedback to assist the driver, an experiment involving five operators with different experiences in driving, was conducted with a test map illustrated in Figure 13.

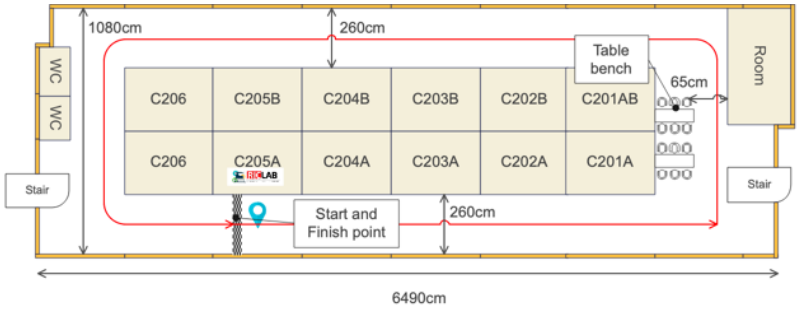

Figure 13. *The testing map for Car-like mobile robot*

The experiment was conducted twice, once with the force feedback steering system and once without. The results are shown in the chart Figure 14 and Figure 15.

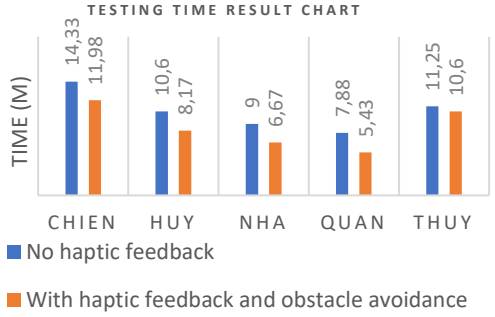

Figure 14. *Testing time result chart*

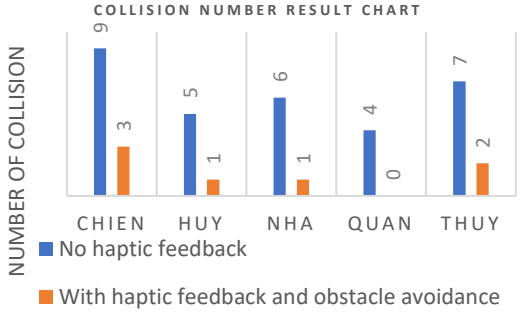

Figure 15. *Collison number results chart*

The experiment demonstrated the effectiveness of the proposed method. The time required for the operator to complete the test was reduced for all 5 drivers, with an average reduction of 8,95%. The number of collisions was also reduced by 77,42%. This was achieved through driver assistance systems such as force feedback steering and obstacle avoidance algorithms that improved the awareness of the operators about the working environment of the robot.

6. Conclusions

In this paper, the enhanced teleoperation system with visual-force feedback and obstacle avoidance for a Car-like mobile robot has been presented. The research calculates and designs the remote control cockpit system, including the force feedback steering mechanism, pedals, mode-switch lever, and display screen with graphics user interface for the mobile robot. By using WAN architecture with MQTT protocol, the teleoperation system has an unlimited control range which is believed to be the weakness of the remote control system. The PF algorithm has been applied to generate the haptic effect of the obstacles in the remote station for the operator due to the visual-force feedback. Successful design and

testing of force feedback on the steering wheel and visual feedback through the user interface were achieved. The results from several tests have shown the effectiveness of the proposed system.

Acknowledgments

This research was implemented at the Robotics and Intelligent Control Laboratory (RIC Lab), Faculty of Electrical and Electronics Engineering, Ho Chi Minh City University of Technology and Education, Vietnam.

Conflict of Interest

The authors declare no conflict of interest.

REFERENCES

[1] S. Bonadies and S. A. Gadsden, "An overview of autonomous crop row navigation strategies for unmanned ground vehicles," *Engineering in Agriculture, Environment and Food*, vol. 12, no. 1, pp. 24-31, 2019, doi: 10.1016/j.eaef.2018.09.001.

[2] M. D. Moniruzzaman, A. Rassau, D. Chai, and S. M. S. Islam, "Teleoperation methods and enhancement techniques for mobile robots: A comprehensive survey," *Robotics and Autonomous Systems*, vol. 150, p. 103973, 2022, doi: 10.1016/j.robot.2021.103973.

[3] T. Bellet *et al.*, "From semi to fully autonomous vehicles: New emerging risks and ethico-legal challenges for human-machine interactions," *Transportation Research Part F: Traffic Psychology and Behaviour*, vol. 63, pp. 153-164, 2019, doi: 10.1016/j.trf.2019.04.004.

[4] I. R. Nourbakhsh, K. Sycara, M. Koes, M. Yong, M. Lewis, and S. Burion, "Human-robot teaming for search and rescue," *IEEE Pervasive Computing*, vol. 4, no. 1, pp. 72-79, 2005, doi: 10.1109/MPRV.2005.13.

[5] N. Murakami *et al.*, "Development of a teleoperation system for agricultural vehicles," *Computers and Electronics in Agriculture*, vol. 63, no. 1, pp. 81-88, 2008, doi: 10.1016/j.compag.2008.01.015.

[6] F. Chen, Y. Huo, J. Zhu, and D. Fan, "A Review on the Study on MQTT Security Challenge," in *2020 IEEE International Conference on Smart Cloud (SmartCloud)*, 6-8 Nov. 2020, pp. 128-133, doi: 10.1109/SmartCloud49737.2020.00032.

[7] M. D. Phung, C. H. Quach, X. Q. Vu, and Q. V. Tran, "Control of a Mobile Robot over the Internet Using CORBA as Communication Architecture," 2010.

[8] D. C. Cuong, L. H. Linh, and H. H. Ngo, "Remote-controlled robot model using computer and radio waves," *TNU Journal of Science and Technology*, 2010.

[9] H. H. Tran and D. T. Tran, "Design of a haptic feedback controller for robot operation," 2022.

[10] A. Junaedy, H. Masuta, K. Sawai, T. Motoyoshi, and N. Takagi, "LPWAN-Based Real-Time 2D SLAM and Object Localization for Teleoperation Robot Control," *Journal of Robotics and Mechatronics*, vol. 33, no. 6, pp. 1326-1337, 2021, doi: 10.20965/jrm.2021.p1326.

[11] F. Panchi, K. Hernández, and D. Chávez, "MQTT Protocol of IoT for Real Time Bilateral Teleoperation Applied to Car-like Mobile Robot," in *2018 IEEE Third Ecuador Technical Chapters Meeting (ETCM)*, 15-19 Oct. 2018, pp. 1-6, doi: 10.1109/ETCM.2018.8580299.

[12] S. M. H. Rostami, A. K. Sangaiah, J. Wang, and X. Liu, "Obstacle avoidance of mobile robots using modified artificial potential field algorithm," *EURASIP Journal on Wireless Communications and Networking*, vol. 2019, no. 1, p. 70, 2019, doi: 10.1186/s13638-019-1396-2.

Tran Duc Thien received the B.S and M.S. degrees in the Department of Electrical Engineering, Ho Chi Minh City University of Technology, Vietnam, in 2010, 2013, and the Ph.D. degree from University of Ulsan in 2020, respectively.
He works as a lecturer with the Department of Automatic Control, Ho Chi Minh City University of Technology and Education (HCMUTE), Vietnam. His research interests include robotics, variable stiffness system, fluid power control, disturbance observer, nonlinear control, adaptive control, and intelligent technique.
Email: thientd@hcmute.edu.vn. ORCID: https://orcid.org/0000-0002-6684-0681

Vo Hoang Quan received the diploma of engineer majoring in automative engineering from the Faculty For High-Quality Training, Ho Chi Minh City University of Technology and Education, Vietnam, in 2023.
He works as a Robotics and Intelligent Control Lab member in the Department of Automatic Control, Ho Chi Minh University of Technology and Education, Vietnam.
His research interests include robotics, mobile robots, automative electrical and electronic systems, and intelligent control.
Email: 2390512@student.hcmute.edu.vn. ORCID: https://orcid.org/0009-0006-1126-6156

Nguyen Trung Kien received the diploma of engineer majoring in automative engineering from the Faculty For High-Quality Training, Ho Chi Minh City University of Technology and Education, Vietnam, in 2023.
He works as a Robotics and Intelligent Control Lab member in the Department of Automatic Control, Ho Chi Minh University of Technology and Education, Vietnam.
His research interests include robotics, mobile robots, automative electrical and electronic systems, and intelligent control.
Email: 2390508@student.hcmute.edu.vn. ORCID: https://orcid.org/0009-0000-6474-8331

Nguyen Thanh Nha received the diploma of engineer majoring in control engineering and automation from the Faculty For High-Quality Training, Ho Chi Minh City University of Technology and Education, Vietnam, in 2023.
He works as a Robotics and Intelligent Control Lab member in the Department of Automatic Control, Ho Chi Minh University of Technology and Education, Vietnam.
His research interests include robotics, parallel robots, nonlinear control, and intelligent control.
Email: 2341104@student.hcmute.edu.vn. ORCID: https://orcid.org/0009-0004-1302-5378